Hindawi
Science and Technology of Nuclear Installations
Volume 2018, Article ID 6378504, 15 pages
https://doi.org/10.1155/2018/6378504

Research Article

Process of Air Ingress during a Depressurization Accident of GTHTR300

Tomoya Shiga, Yudai Tanaka, and Tetsuaki Takada

Mechanical Engineering Course, Graduate School of Engineering, University of Yamanashi, 4-3-11 Takeda, Kofu, Yamanashi 400-8511, Japan

Correspondence should be addressed to Tetsuaki Takada; ttakeda@yamanashi.ac.jp

Received 30 March 2018; Revised 9 June 2018; Accepted 31 July 2018; Published 2 September 2018

Academic Editor: Hidemasa Yamano

A depressurization accident is the design-basis accidents of a gas turbine high temperature reactor, GTHTR300, which is JAEA's design and one of the Very-High-Temperature Reactors (VHTR). When a primary pipe rupture accident occurs, air is expected to enter the reactor core from the breach and oxidize in-core graphite structures. Therefore, it is important to know a mixing process of different kinds of gases in the stable and unstable density stratified fluid layer. In order to predict or analyze the air ingress phenomena during the depressurization accident, we have conducted an experiment to obtain the mixing process of two component gases and the characteristics of natural circulation. The experimental apparatus consists of a storage tank and a reverse U-shaped vertical rectangular passage. One side wall of the high temperature side vertical passage is heated and the other side wall is cooled. The other experimental apparatus consists of a cylindrical double coaxial vessel and a horizontal double coaxial pipe. The outside of the double coaxial vessel is cooled and the inside is heated. The results obtained in this study are as follows. When the primary pipe is connected at the bottom of the reactor pressure vessel, onset time of natural circulation of air is affected by not only molecular diffusion but also localized natural convection. When the wall temperature difference is large, onset time of natural circulation of air is strongly affected by natural convection rather than molecular diffusion. When the primary pipe is connected at the side of the reactor pressure vessel, air will enter the bottom space in the reactor pressure vessel by counter-current flow at the coaxial double pipe break part immediately. Afterward, air will enter the reactor core by localized natural convection and molecular diffusion.

1. Introduction

One of the next-generation nuclear plants is a Very-High-Temperature Reactor (VHTR). The VHTR has strong interests of development worldwide. In addition to broad economical appeal resulting from unique high temperature capability, the reactor provides inherent and passive safety. The Japan Atomic Energy Agency (JAEA) has successfully built and operated the 30 MWt High Temperature engineering Test Reactor (HTTR) and is now pursuing design and commercial systems such as the 300 MWe Gas Turbine High Temperature Reactor 300 (GTHTR300). Also, in order to deploy a commercial Gas Turbine High Temperature Reactor 300 for Cogeneration (GTHTR300C) in around 2030, JAEA is now carrying out design study [1, 2].

When a double coaxial pipe connecting a reactor and a Gas Turbine Generator (GTG) module breaks, air is expected to enter the reactor core from the breach. The depressurization accident is one of the design-basis accidents of the GTHTR300. When the depressurization accident occurs, air is expected to enter the reactor core from breach and oxidize in-core graphite structures. Air ingress process in the VHTR is known to follow two sequential phases. Density of the gas mixture in the reactor gradually increases as air enters by the molecular diffusion and natural convection of the gas mixture in the first stage of the accident. Finally, the second stage of the accident starts after the natural circulation of air occurs suddenly throughout the entire reactor. The natural circulation of air suddenly occurs as once sufficient buoyancy is established [3]. On the other hand, under specific boundary condition, the onset time for producing natural circulation is short [4, 5].

A related study investigated the air ingress process and development of a passively safe technology to prevent air

ingress. In order to clarify the safety characteristics of the GTHTR300C in a pipe rupture accident, a preliminary analysis of air ingress was performed [6]. The previous paper described the influence of local natural circulation in parallel channels on the air ingress process during a primary pipe rupture accident in the VHTR [7]. The duration of the first stage of the air ingress process was also discussed with analytical results of the reverse U-shaped passage with parallel channels.

During depressurization accident in the VHTR, localized natural convection will occur in the space between the reactor pressure vessel and the permanent reflector. The Grashof number in natural circulation flow is based on the density difference between hot and cold leg. The natural circulation flow rate is determined by the point where the buoyancy and the pressure loss of the flow path are balanced. For example, the range of Rayleigh number based on space width is about $0 < Ra_d < 5.0\times10^9$ in the HTTR. Therefore, the amount of transported oxygen depends not only on molecular diffusion but also on natural convection, and it is important to know a mixing process of different kinds of gases in the stable or unstable stratified fluid layer. In particular, it is also important to examine the influence of localized natural convection and molecular diffusion on the mixing process from a safety viewpoint.

Previous studies focused mostly on molecular diffusion and natural circulation of the two-component gas mixture in a reverse U-shaped tube and in a simple test model of the HTTR [8]. In order to investigate the basic features of the flow behavior of multicomponent gas mixtures consisting of helium (He), nitrogen (N_2), oxygen (O_2), carbon dioxide (CO_2), carbon monoxide (CO), etc., experimental and numerical studies were performed to study the combined phenomena of molecular diffusion and natural circulation of the multicomponent gas mixtures along with the graphite oxidation reaction in a reverse U-shaped tube [9]. The numerical results were in good agreement with the experimental results in regard to the density change of the gas mixture, the molar fraction change of the gas species, and onset time of natural circulation of air. Furthermore, the objectives of these studies were to investigate the air ingress process and to develop a safe passive technology for the prevention of air ingress [3]. Recently, a density-gradient driven air ingress stratified flow was analyzed using CFD code for the Next-Generation Nuclear Plant (NGNP), which is a US designed VHTR [10] (Oh, et al., 2010). Authors have reported on the mixing process of two component gases through natural convection and molecular diffusion in a stable stratified fluid layer [11]. According to the report, the mixing process through molecular diffusion in the vertical stratified fluid layer was significantly affected by the localized natural convection induced by a slight temperature difference between both vertical walls. The report described the process of air ingress during the first stage of a primary pipe rupture accident, and provided experimental results regarding the influence of localized natural circulation in the parallel channels on the air ingress process. Localized natural convection may affect the onset time of natural circulation [12–14]. In order to predict or analyze the air ingress phenomena during the depressurization accident in the VHTR, it is important to examine the influence of localized natural convection and molecular diffusion on the mixing process.

In general, mixing processes of two component gases in a vertical stable stratified fluid layer are governed by molecular diffusion. When a stable stratification is formed in a vertical slot with two component gases which have different densities, the rate of transportation will be different, as determined by mutual diffusion coefficient. On the other hand, it is expected that natural convection will occur in vertical slot when one sidewall is heated and the other sidewall is cooled. When a stable stratification is formed with the two component gases and two vertical parallel walls of the slot are kept at different temperature, the transport process of the gases becomes more complex. In this case, the heavy gas diffuses into the light gas. In addition to that these gases will also be transported by natural convection. Both phenomena may occur at the same time during the air ingress process of the depressurization accident. Molecular diffusion and natural convection will occur simultaneously in the annular passage between the inner barrel and the water-cooled jacket [3]. The range of the Rayleigh number base on the width of the annular passage is about $0 < Ra_d < 3.26\times10^5$ and $Ra_d < 1.56\times10^6$, respectively. The Rayleigh number based on the width of the annular passage of the HTTR or the GTHTR300C will be bigger than two digits of the Ra number based on the width of the simulated apparatus. Therefore, scaling analysis was carried out to find out which phenomena is dominant in the mixing process of two component gases in a vertical stable stratified fluid layer. In this study, we have carried out experiments and obtained the mixing process of two component gases and flow characteristics of localized natural convection. We also investigated the air ingress process when the horizontal double coaxial pipe ruptures.

2. Experiment on Two-Component Gas Mixing Process of Reverse U-Shaped Vertical Rectangular Channel

2.1. Experimental Apparatus [15] (Tanaka & Takeda, 2016). Figure 1 shows the schematic drawing of an experimental apparatus of vertical rectangular channel. The experimental apparatus consists of a reverse U-shaped vertical slot and a storage tank. One side slot consists of the heated and cooled walls. The other side slot consists of the two cooled walls. The dimensions of the vertical slots are 598 mm in height, 208 mm in depth, and 70 mm in width. Each two vertical slots were connected and were a reverse U-shaped passage. The dimensions of the connecting passage were 16 mm in height, 106 mm in depth, and 210 mm in length. The storage tank was connected to the lower part of the reverse U-shaped passage. The dimensions of the storage tank were 248 mm in height, 398 mm in depth, and 548 mm in width. The reverse U-shaped passage and the storage tank were separated by a partition plate.

Figure 2 shows the high temperature side slot of the reverse U-shaped passage. A stainless sheath heater and a

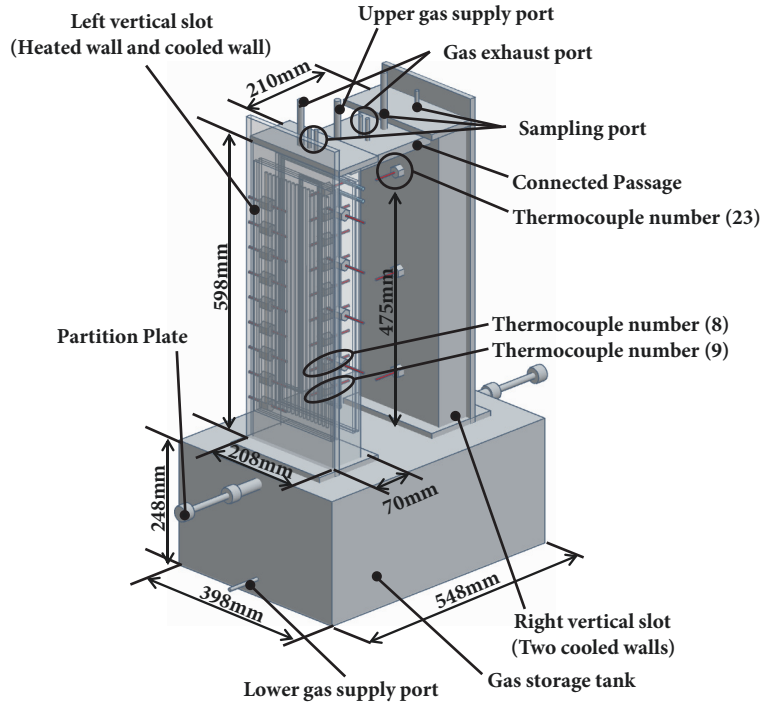

Figure 1: Experimental apparatus of reverse U-shaped vertical rectangular channel.

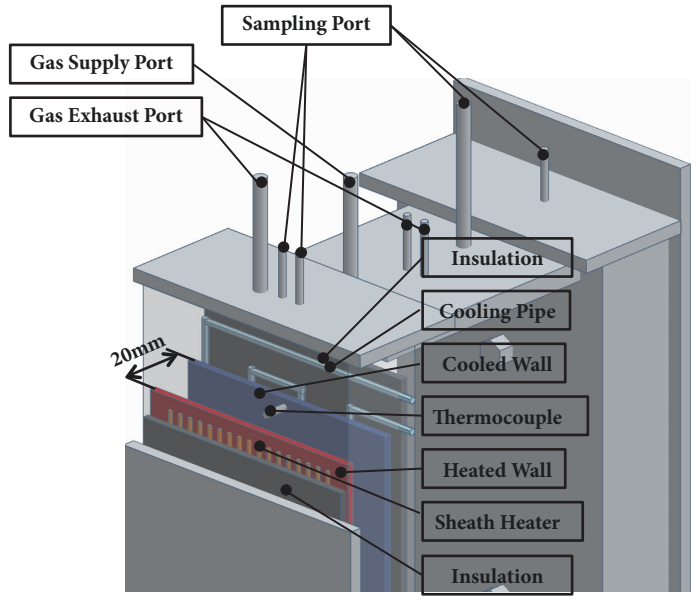

Figure 2: Schematic of high temperature side slot of reverse U-shaped passage.

water cooling pipe made of copper were attached to the heated wall and the cooled wall, respectively. These walls were covered by an insulator which was 30 mm in thickness. The dimension of the heated walls was 500 mm in height and 200 mm in width. The dimension of the low temperature side slot was the same as the high temperature side slot. The distance between the heated wall and cooled wall has been set to 20 mm. The wall and gas temperature were measured by a K-type thermocouple. Considering the errors induced by the thermocouples, the scanner junction, and the DVM accuracy, the entire accuracy of the temperature measurement was within ±0.5 K. The temperature measurement position is provided in Table 1 and Figure 3.

2.2. Experimental Method. The experimental procedure is as follows. The partition plate between the reverse U-shaped passage and the storage tank is closed. The reverse U-shaped passage is filled with a lighter gas, which is helium for

Table 1: Position of temperature measurement.

Gas temperature of high temperature side			Heated wall temperature		
No.	Distance from bottom [mm]	Diameter	No.	Distance from bottom [mm]	Diameter
1	490	φ1	10	440	φ1
2	440	φ1	11	390	φ1
3	390	φ1	12	340	φ1
4	340	φ1	13	290	φ1
5	290	φ1	14	240	φ1
6	240	φ1	15	190	φ1
7	190	φ1	16	140	φ1
8	140	φ1	17	90	φ1
9	90	φ1	18	40	φ1
Cooled wall temperature			Gas temperature of low temperature side		
No.	Distance from bottom [mm]	Diameter	No.	Distance from bottom [mm]	Diameter
19	440	φ1	23	475	φ1.6
20	340	φ1	24	275	φ1.6
21	240	φ1	25	75	φ1.6
22	140	φ1	—	—	—

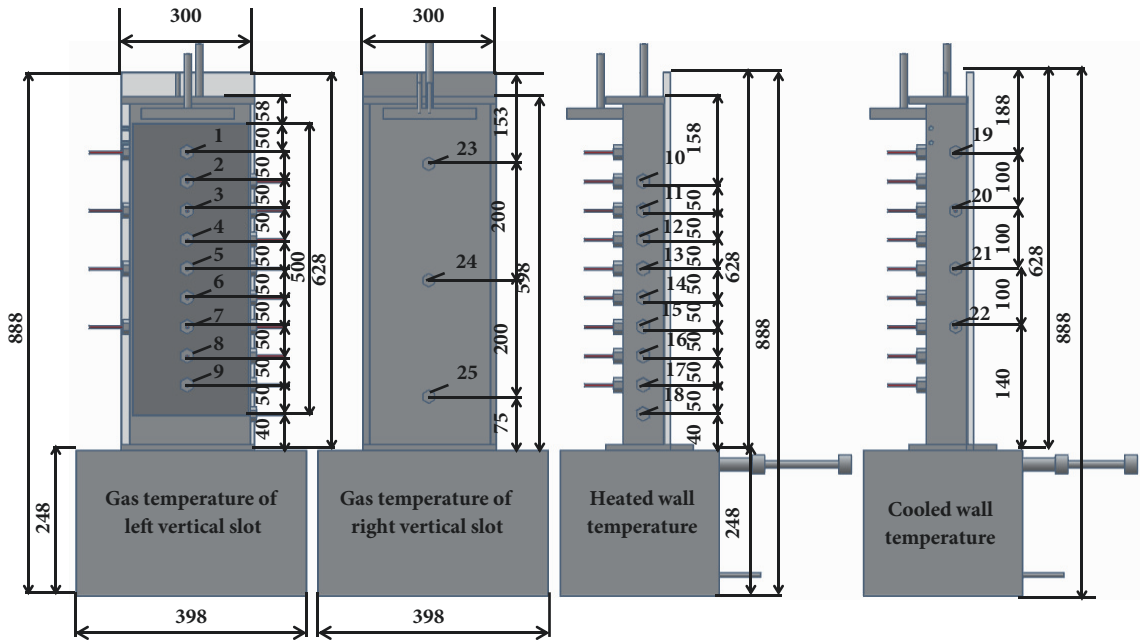

Figure 3: Position of temperature measurement.

example, and the storage tank is filled with heavier gas, which is nitrogen, air, and argon for example. The one side of copper plate in the high temperature side slot is heated and the other side plate is cooled by water. As the copper plate was heated until set temperature, the gas pressure in the slots and the storage tank was kept at the atmospheric pressure. After confirming that the temperature of the various points in the apparatus reached the steady state condition, the partition plate was opened. The working fluids used five kinds of gases which are helium (He), nitrogen (N_2), argon (Ar), neon (Ne), and air (Air). The combinations of two component gases are set to He/Air, He/N_2, Ne/Ar, and N_2/Ar. The combinations of density ratios are 1.38/10, 1.43/10, 5/10, and 7/10. Temperature difference between the heated wall and cooled wall is set to 30, 50, and 70 K.

2.3. Experimental Results and Discussion. Figures 4 and 5 show the temperature result of He/N_2 experiment. The gas temperature change with time in the high temperature side slot is shown in Figure 4. The gas temperature change with time in the low temperature side slot is shown in Figure 5. The temperature difference between the heated wall and cooled wall was set to 70 K.

Table 2: Onset time of natural circulation.

△T[K]	He/Air	He/N_2	Ne/Ar	N_2/Ar
30	85 min	93 min	135 min	175 min
50	65 min	70 min	110 min	132 min
70	60 min	50 min	—	120 min
density ratio	1.38/10	1.43/10	5/10	7/10

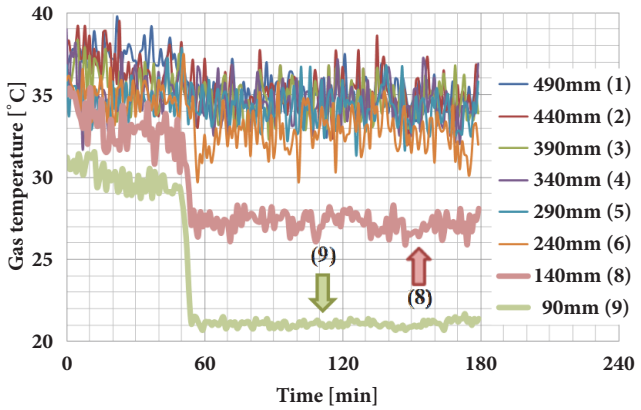

Figure 4: Gas temperature change with time in high temperature side slot (He/N_2).

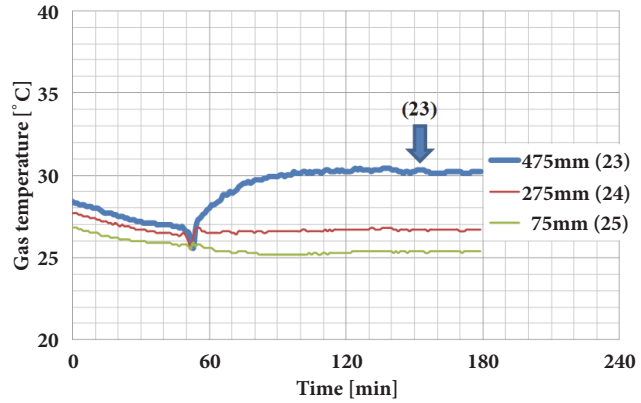

Figure 5: Gas temperature changes with time in low temperature side slot (He/N_2).

As shown in Figure 4, the gas temperature fluctuates during the early stage of the experiment (within 50 min). It seems to be probable that localized natural convection produces in the high temperature side slot [16]. The gas temperature change at number (8) and (9) in the high temperature side slot was suddenly decreased at about 50 minutes after the start of the experiment (opening of the partition plate). On the other hand, the gas temperature change at number (23) in the low temperature side slot was suddenly increased at the same time. Such gas temperature change will be explained as follows. The density difference between the high temperature side slot and the low temperature side slot becomes small just after the start of the experiment. The heavy gas diffuses into both slots with elapsing time. Meantime, as shown in Figure 6, the localized natural convection produces in the high temperature side slot. Therefore, the density difference between the high temperature side slot and the low temperature side slot will increase with elapsing time. Finally, as the buoyancy becomes increased enough, natural circulation through the reverse U-shaped passage produces suddenly. Thus, the gas temperature at the lower part of the high temperature side slot increases and the gas temperature at upper part of the low temperature side slot decreases just after the onset of natural circulation.

Rayleigh number, Grashof number, and Prandtl number are defined as the following equations:

$$\mathrm{Ra_d} = \mathrm{Gr} \cdot \mathrm{Pr} \tag{1}$$

$$\mathrm{Gr_d} = \frac{\left(g\beta\left(T_w - T_e\right)D_e^{\,3}\right)}{\nu^2} \tag{2}$$

$$\mathrm{Pr} = \frac{\mu C_p}{\lambda} \tag{3}$$

Here, g is the gravitational acceleration [m/s^2], β is the thermal expansion coefficient [1/K], T_w is the average temperature of the heated flat plate in the left side slot [K], T_e is the average gas temperature in the left side slot [K], and D_e is the equivalent diameter [m]. The width of the vertical slot was used as the equivalent diameter. ν is kinematic viscosity [m^2/s]. μ is viscosity coefficient [kg/m·s], C_p is constant pressure specific heat [J/kg·K], and λ is thermal conductivity [W/m·K].

Table 2 shows the onset time of natural circulation under various experimental conditions. Table 3 shows the Rayleigh number based on the width of the high temperature side channel. As shown in Table 3, it is possible that the flow regime of natural convection changes conduction regime to transition or boundary layer regime in the He/Air and He/N_2 experiment [17]. Therefore, not only molecular diffusion but also localized natural convection will affect the onset time of natural circulation. There is a mutual diffusion coefficient as an index characterizing molecular diffusion. D_{AB} is the mutual diffusion coefficient of gas A in gas B. Gas A is heavy gas; gas B is light gas. D_{AB} is obtained by literature [18]. Table 4 shows the mutual diffusion coefficient under the various experimental condition. Numbers in parentheses are the gas temperature in the high temperature side slot. It can be seen that the mutual diffusion coefficient of two component gases depends on the gas temperature in the high temperature side slot.

As shown in Table 2, the onset time of natural circulation decreased with an increasing temperature difference for each combination of gases. The range of the Rayleigh

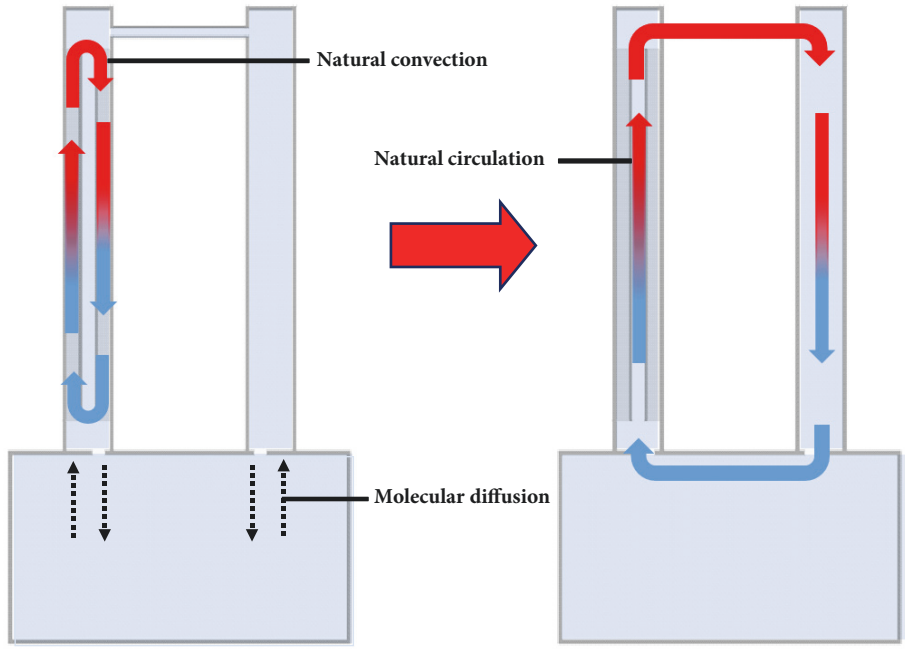

Figure 6: Illustration of change of flow pattern.

Table 3: Rayleigh number based on the width of the high temperature side slot.

△T[K]	He/Air(×10^4)	He/N_2(×10^4)	Ne/Ar (×10^4)	N_2/Ar (×10^4)
30	0.0226≤ Ra_d ≤1.03	0.0243≤ Ra_d ≤1.49	0.358≤ Ra_d ≤1.91	2.09≤ Ra_d ≤2.43
50	0.0364≤ Ra_d ≤1.54	0.0436≤ Ra_d ≤2.54	0.554≤ Ra_d ≤2.73	3.18≤ Ra_d ≤3.58
70	0.0590≤ Ra_d ≤2.63	0.0598≤ Ra_d ≤3.06	—	4.04≤ Ra_d ≤4.32

Table 4: Mutual diffusion coefficient of two component gases.

△T[K]	He/Air[cm^2/s]	He/N_2[cm^2/s]	Ne/Ar[cm^2/s]	N_2/Ar[cm^2/s]
30	**0.721** (304 K)	**0.696** (301 K)	**0.304** (296 K)	**0.191** (298 K)
50	**0.737** (308 K)	**0.700** (302 K)	**0.311** (300 K)	**0.196** (302 K)
70	**0.721** (304 K)	**0.720** (307 K)	—	**0.194** (301 K)

number based on the width of the high temperature side slot is shown in Table 3. The Rayleigh number increased with an increasing temperature difference. The influence of natural convection increased with an increase in the temperature difference between the heated and cooled walls. Thus, the onset time of natural circulation decreased. When the temperature difference was 30 and 50 K, the onset time of natural circulation decreased with an increase in the diffusion coefficient. However, the onset time of natural circulation for He/N_2 was shorter than that for He/Air regardless of the diffusion coefficient when the temperature difference was 70 K. The Rayleigh number for He/N_2 is larger than that for He/Air as shown in Table 3. Therefore, the onset time of natural circulation depended more on molecular diffusion than the strength of localized natural convection when the temperature difference was small. On the other hand, the onset time of natural circulation depended not only on molecular diffusion but also on localized natural convection when the temperature difference was large.

Figures 7, 8, and 9 show the gas temperature change with time in the high temperature side slot under the condition of temperature differences of 30 K, 50 K, and 70 K, respectively. The onset time of natural circulation becomes shorter as the mutual diffusion coefficient becomes large in the He/Air and He/N_2 experiment under the condition of the temperature differences of 30 K and 50 K. However, in the case where the He/Air and He/N_2 experiment is under the condition of the temperature difference of 70 K, the onset time of natural circulation is shorter for He/N_2 experiment compared with He/Air experiment. The Rayleigh number of the He/N_2 experiment becomes large compared with the Rayleigh number of the He/Air experiment. This result shows that the influence of localized natural convection is greater than molecular diffusion when temperature difference is large.

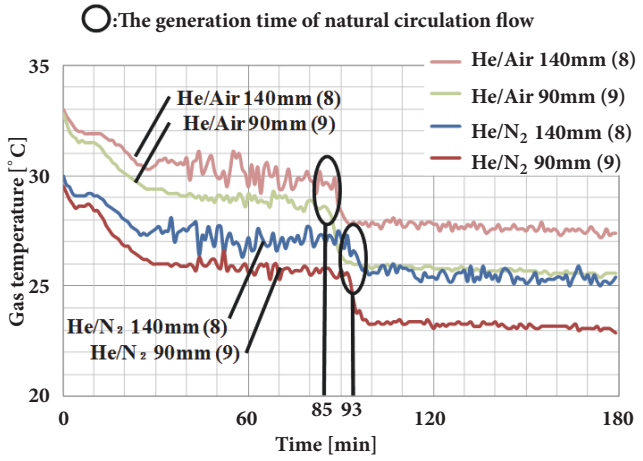

Figure 7: Gas temperature changes in high temperature side slot (T/C Numbers 8 and 9) when wall temperature difference is set to 30 K.

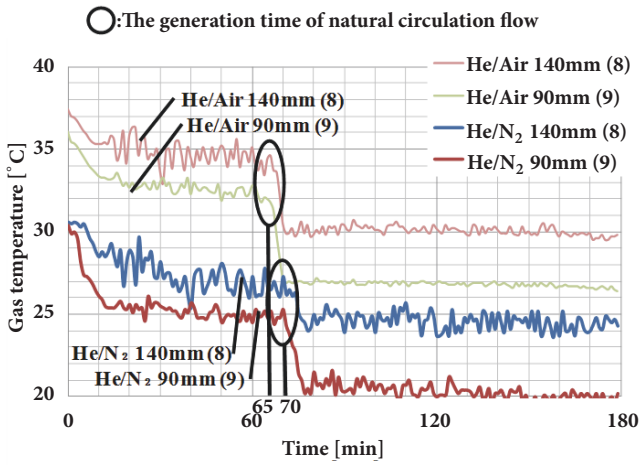

Figure 8: Gas temperature changes in high temperature side slot (T/C Numbers 8 and 9) when wall temperature difference is set to 50 K.

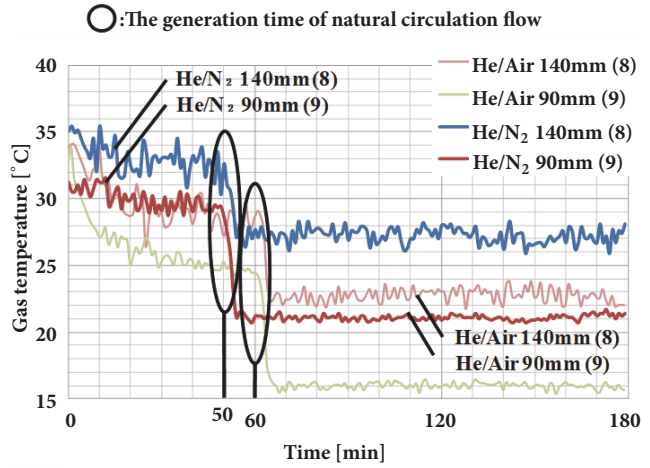

Figure 9: Gas temperature changes in high temperature side slot (T/C Numbers 8 and 9) when wall temperature difference is set to 70 K.

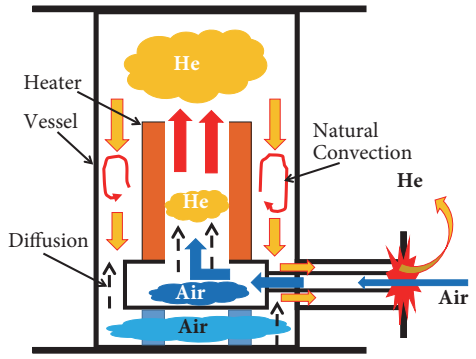

Figure 10: Apparatus simulated horizontal pipe rupture accident in GTHTR300.

3. Experiment on Gas Mixing Process and Natural Circulation Flow at the Time of Horizontal Piping Rupture of Double Coaxial Cylinder

3.1. Experimental Apparatus. The other experiment for a horizontal pipe break case is planned using apparatus which is shown in Figure 10. Air ingress scenario in the case of the horizontal pipe break of the GTHTR300C is as follows. After the pipe ruptures, air will flow into the bottom part of the reactor pressure vessel by the counter-current flow. The density stratified fluid layer will be formed. Buoyancy will produce between the hot and cold legs. As the buoyancy will be small, the natural circulation flow will not produce under the condition of this density distribution. Thus, air will be transported to the reactor core by mainly molecular diffusion. However, from the results obtained in these experiment, air will be transported to the reactor core by the localized natural convection. In the configuration of the HTTR, a vertical channel existed between the reactor pressure vessel and the pipe rupture part. So, it needed much time to onset of natural circulation of air. In the configuration of the GTHTR300C, the vertical path does not exist between the reactor pressure vessel and the pipe rupture part. Therefore, air may be transported to the reactor core earlier. The onset time of the natural circulation of air and the amount of infiltrating air during the accident will be greatly affected by the produced position and strength of the localized natural convection in the pressure vessel. If the localized natural convection occurs inside the channel, it is difficult to estimate not only the density change of gas mixture but also the onset time of natural circulation through the reactor. Anyway, after the time elapses, the natural circulation may occur suddenly. In order to research the mixing process of two component gases when the horizontal primary pipe of the GTHTR300C is ruptured, experiment and analysis are planned.

Figure 11 shows the schematic drawing of an experimental apparatus of double coaxial cylinder. The experimental apparatus consists of a double coaxial cylinder and horizontal

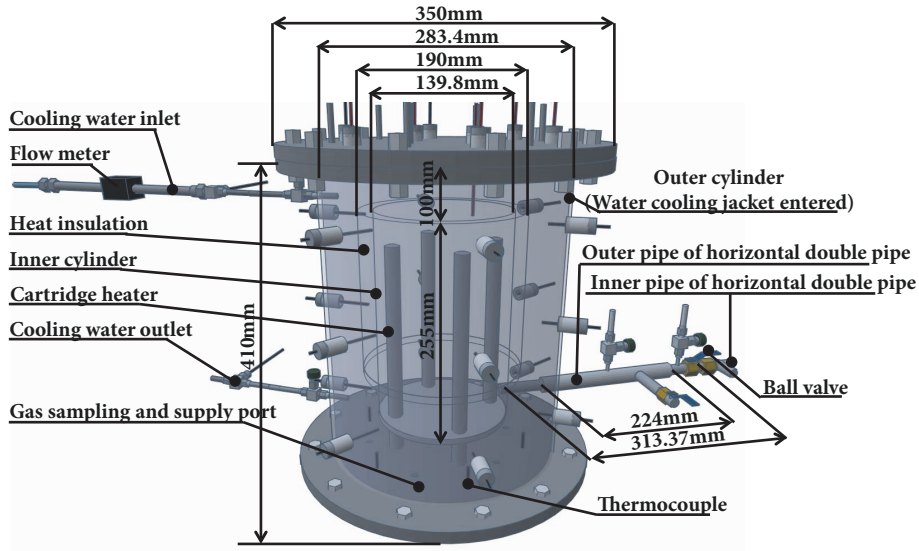

Figure 11: Experimental apparatus of double coaxial cylinder.

double coaxial pipe. The dimensions of the outer cylinder of the double coaxial cylinder are 410 mm in height, 283.4 mm in outer diameter, and 267.4 mm in inner diameter. The inner pipe of the horizontal double coaxial pipe is connected to the inner cylindrical lower part, and the dimensions thereof are 313.4 mm in length, 21.7 mm in outer diameter, and 17 mm in inner diameter. The annular flow channel of the horizontal double coaxial pipe is connected to the outer cylinder, and the dimension thereof is 224 mm in length, 34 mm in outer diameter, and 30 mm in inner diameter. A ball valve was installed in the inner pipe and the outer pipe of the horizontal double coaxial pipe. Four cartridge heaters were installed in the inner cylinder and heated. The standard of the cartridge heater is 300 mm in length, 12.8 mm in outer diameter, 170 mm in effective heating portion, rated voltage of 100 V, and rated capacity of 100 W. A water cooling jacket was inserted into the outer cylinder and cooled. In order to prevent heat radiation, a heat insulating material (round furnace, ceramic type) with a height of 200 mm and a thickness of 23.5 mm was installed on the inner cylinder. The top and bottom of the experimental apparatus were covered with a lid to close the apparatus. One port with an outer diameter of 6.35 mm was used as a gas supply port.

A K-type thermocouple was used for temperature measurement. The thermocouple installation positions are shown in Figures 12–14 and Table 5. The temperature measurement error accuracy of this thermocouple is ± 1.5 K. The thermocouple was inserted through a pore of 1.2 mm in diameter of a compression fitting provided on the outer cylinder. Six thermocouples were installed at the 5 mm position from the outer cylinder (thermocouples numbers 1, 2, 7, 8, 13, and 14). Six thermocouples were installed at the 16.5 mm position from the outer cylinder (thermocouples numbers 3, 4, 9, 10, 15, and 16). Six thermocouples were installed at the 28 mm position from the outer cylinder (thermocouples numbers 5, 6, 11, 12, 17, and 18). A total of 18 thermocouples were installed and gas temperature changes in the outer channel were measured. In order to measure the gas temperature at the bottom of the experimental apparatus, 6 thermocouples were installed at 25 mm from the bottom of the apparatus (thermocouples numbers 21-26). In order to measure the gas temperature at the top of the experimental apparatus, 8 thermocouples were installed at 410 mm from the bottom of the apparatus (thermocouples numbers 31-38). Two thermocouples for cooling water temperature measurement were installed at the water cooling jacket entrance. Heater temperature was measured with built-in thermocouple.

For measurement of the gas concentration, an ultrasonic gas concentration meter was used. The gas concentration measurement positions are shown in Figures 12–14 and Table 6. Gas was sampled with a microtube pump from the sampling port provided in the bottom part, upper part, and horizontal double coaxial pipe of the experiment apparatus, and the concentration was measured. A constant temperature type thermal anemometer was used to measure the gas flow velocity. Figure 12 and Table 7 show the measurement position of the gas flow velocity. The flow velocity was measured by attaching an anemometer to the valve installed on the horizontal dual coaxial tube.

3.2. Experimental Method. Experimental procedure is as follows. The experimental apparatus is filled with helium gas. The inner cylinder is heated, and the outer cylinder is cooled by the water cooling jacket. After the heater temperature is reached at steady state, the valves attached to the horizontal double coaxial pipe are opened at the same time. During the experiment, the temperature and mole fraction of two component gases are measured. The flow velocity at the inlet and outlet of the horizontal double coaxial pipe is also measured. Heat input is 36 W (1.22 kW/m^2), 144 W (4.89 kW/m^2), and 324 W (11.0 kW/m^2).

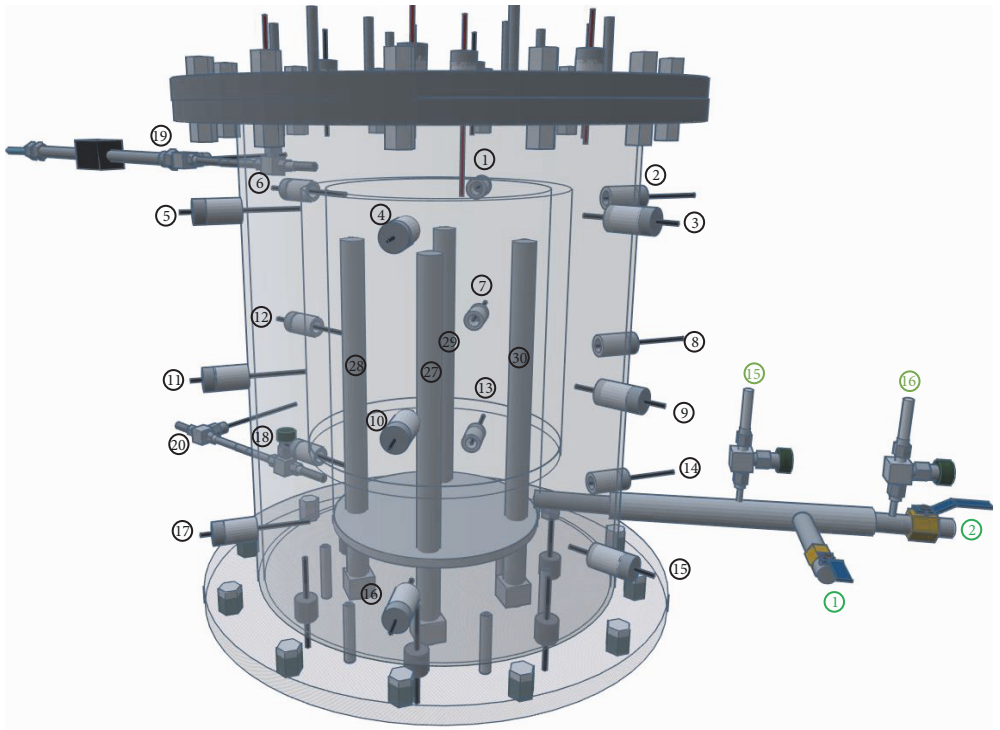

○ :Gas temperature measurement position
○ : Gas concentration measurement position
○ : Gas flow velocity measurement position

Figure 12: Measurement positions of temperature, gas concentration, and flow velocity.

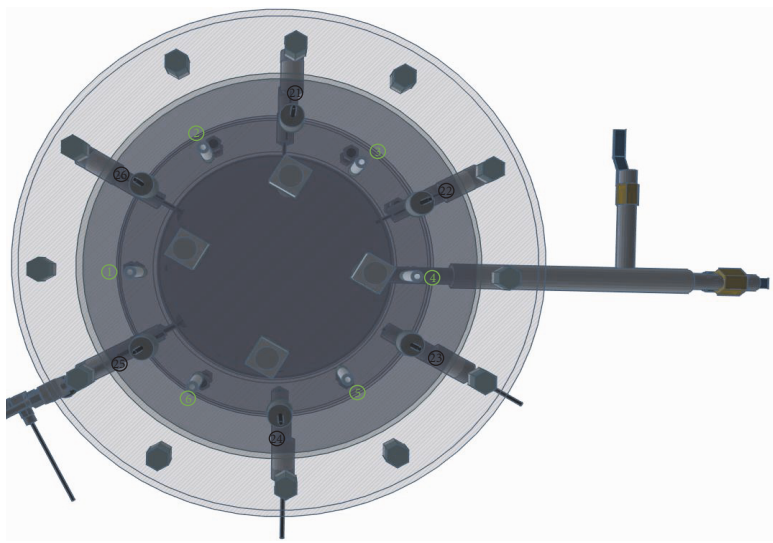

○ :Gas temperature measurement position
○ : Gas concentration measurement position
○ : Gas flow velocity measurement position

Figure 13: Measurement position of temperature, gas concentration, and flow velocity (bottom view).

Table 5: Positions of temperature measurement.

No.	Distance from bottom [mm]	Distance from outer cylinder [mm]	Diameter
	Gas temperature in the experimental apparatus of double coaxial cylinder		
1	337.5	5	$\varphi 1$
2	337.5	5	$\varphi 1$
3	337.5	16.5	$\varphi 1$
4	337.5	16.5	$\varphi 1$
5	337.5	28	$\varphi 1$
6	337.5	28	$\varphi 1$
7	205	5	$\varphi 1$
8	205	5	$\varphi 1$
9	205	16.5	$\varphi 1$
10	205	16.5	$\varphi 1$
11	205	28	$\varphi 1$
12	205	28	$\varphi 1$
13	72.5	5	$\varphi 1$
14	72.5	5	$\varphi 1$
15	72.5	16.5	$\varphi 1$
16	72.5	16.5	$\varphi 1$
17	72.5	28	$\varphi 1$
18	72.5	28	$\varphi 1$
21	25	38.7	$\varphi 1$
22	25	38.7	$\varphi 1$
23	25	38.7	$\varphi 1$
24	25	38.7	$\varphi 1$
25	25	38.7	$\varphi 1$
26	25	38.7	$\varphi 1$
31	410	19.7	$\varphi 1$
32	410	19.7	$\varphi 1$
33	410	19.7	$\varphi 1$
34	410	19.7	$\varphi 1$
35	410	19.7	$\varphi 1$
36	410	19.7	$\varphi 1$
37	410	83.7	$\varphi 1$
38	310	83.7	$\varphi 1$
	Temperature of cooling water and cartridge heater		
19	Cooling water inlet		$\varphi 1$
20	Cooling water outlet		$\varphi 1$
27	Cartridge heater 1		$\varphi 1$
28	Cartridge heater 2		$\varphi 1$
29	Cartridge heater 3		$\varphi 1$
30	Cartridge heater 4		$\varphi 1$

3.3. Preliminary Experimental Results and Discussion. Figures 15–17 show gas temperature changes under the condition of the heat input of 324 W. The horizontal axis shows the elapsed time and the vertical axis shows the gas temperature. Symbols show the gas temperature at the specific points (distance from the outer cylinder and the thermocouple number). As shown in Figure 15, the gas temperature fluctuation near the inner cylinder is ± 2.0 K during the experiment. On the other hand, the gas temperature fluctuation near the outer cylinder is ± 0.5 K. Therefore, it was found that the temperature fluctuation increases from the outer cylinder toward the inner cylinder. In addition, the gas temperature difference between the vicinity of the inner and outer cylinder is about 15 to 30 K. From the results obtained, the localized natural convection will occur between the inner and outer cylinders. The gas temperature fluctuation near the wall can be seen when the natural convection produced in the vertical wall with different temperature. After starting the experiment, the gas temperature near the outer cylinder decreased. A temperature difference is generated between the

Table 6: Sampling positions of gas mixture.

Gas concentration in the experimental apparatus of double coaxial cylinder		
No.	Distance from bottom [mm]	Pitch circle diameter [mm]
1	0	190
2	0	190
3	0	190
4	0	190
5	0	190
6	0	190
7	410	228
8	410	228
9	410	228
10	410	228
11	410	228
12	410	228
13	410	100
14	410	100
15	An annular flow channel of horizontal double coaxial pipe	
16	Inner pipe flow channel of horizontal double coaxial pipe	

Table 7: Positions of velocity measurement.

Gas flow velocity in the experimental apparatus of double coaxial cylinder	
No.	Installation position of anemometer
1	Gas inlet and outlet of annular flow channel of horizontal double coaxial pipe
2	Gas inlet and outlet of inner pipe flow channel of horizontal double coaxial pipe

gas temperature in the vicinity of the inner cylinder and the gas temperature in the vicinity of the outer cylinder. As shown in Figures 16 and 17, however, the temperature fluctuation and the temperature difference decrease from the upper part to the lower part of the apparatus. Therefore, the strength of the localized natural convection generated between the inner and outer cylinders differs from the upper part to the lower part of the apparatus.

Consider the change of the flow region of the convection in the apparatus. Table 8 shows the Rayleigh number of the side and top spaces in the apparatus. The equivalent diameter of the side space is the width between the inner diameter and the outer diameter of the coaxial double cylinder. The equivalent diameter of the top space is from the upper surface of the inner cylinder to the upper lid. Rayleigh number which is filled with helium becomes of minimum value and the Rayleigh number which is filled with air becomes of maximum value. This is because the density of air is about 7 times of the density of helium. When the apparatus is filled with helium, the Rayleigh number will be lower than 10^3. Therefore, the region of the localized natural convection becomes conduction regime [17]. On the other hand, when the apparatus is filled with air, the Rayleigh number will exceed 10^4. Therefore, the region of the localized natural convection becomes transition or boundary layer regime.

Figure 18 shows the mole fraction change of air under the condition of the heat input of 324 W. The horizontal axis indicates the elapsed time after the valve opening. The measurement range of an ultrasonic concentration meter for helium gas is from 0 to 50%. Therefore, the solid lines show the mole fraction of air. Figure 19 shows the velocity at the outlet of the outer passage of the double coaxial pipe. From the results obtained in the experiment, air ingress process will be explained as follows. After the valve was opened, the mole fraction of air in the inner pipe of the horizontal double coaxial pipe increased sharply. Air flows into the cylinder from the inner pipe of the horizontal double coaxial pipe. On the other hand, air flows into the cylinder from the outer pipe of the horizontal double coaxial pipe by the counter-current flow. Helium which filled the bottom part of the cylinder will be released to the outside of the cylinder. This condition will be terminated immediately. The mole fraction of air in the outer pipe of the horizontal double coaxial pipe also increased from 0.5 to 0.6. During this time air will be diffused into the cylinder. Afterward the mole fraction change of air decreased and then it increased again. As shown in Figure 18, the mole fraction change of air at the point of (15) decreased at about 20 minutes. Thus, the natural circulation will be generated through the cylinder. The mole fraction of air in the other measurement points increased from 0.5 to 0.6 during the period from 20 to 30 minutes after the valve was opened. As we measured the flow velocity at the outlet of the outer pipe of the double coaxial pipe, we obtained the velocity signal. The velocity

Table 8: Rayleigh number ($\times 10^4$) of the side and top spaces in the apparatus.

Heat input [W]	Distance from the bottom [mm]			
	72.5 (Representative length = 33 mm)	205 (Representative length = 33 mm)	337.5 (Representative length = 033 mm)	410 (Representative length = 139.8 mm)
36	$0.003 \leq Ra_d \leq 0.32$	$0.015 \leq Ra_d \leq 1.24$	$0.023 \leq Ra_d \leq 2.63$	$3.00 \leq Ra_d \leq 219$
144	$0.012 \leq Ra_d \leq 0.87$	$0.040 \leq Ra_d \leq 2.67$	$0.055 \leq Ra_d \leq 5.24$	$8.13 \leq Ra_d \leq 470$
324	$0.014 \leq Ra_d \leq 1.63$	$0.064 \leq Ra_d \leq 4.31$	$0.085 \leq Ra_d \leq 7.82$	$15.0 \leq Ra_d \leq 879$

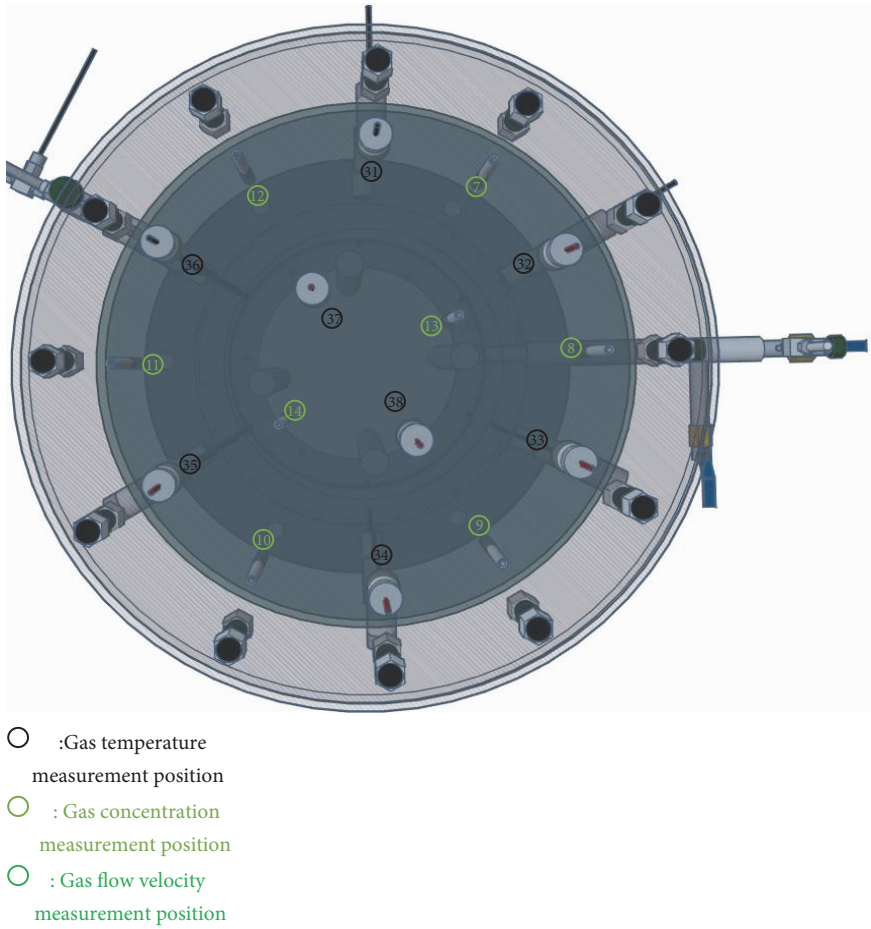

Figure 14: Measurement position of temperature, gas concentration, and flow velocity (top view).

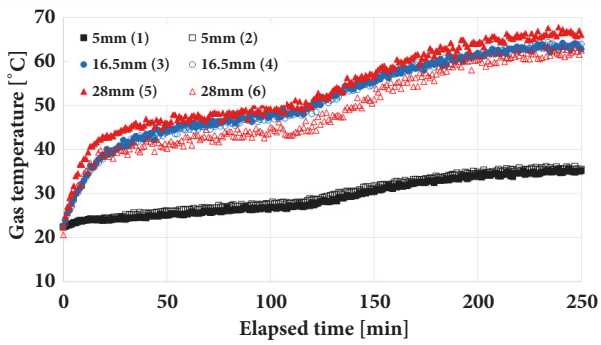

Figure 15: Gas temperature change between inner and outer cylinders (heat input is 324 W). (Distance from bottom of apparatus = 337.5 mm.)

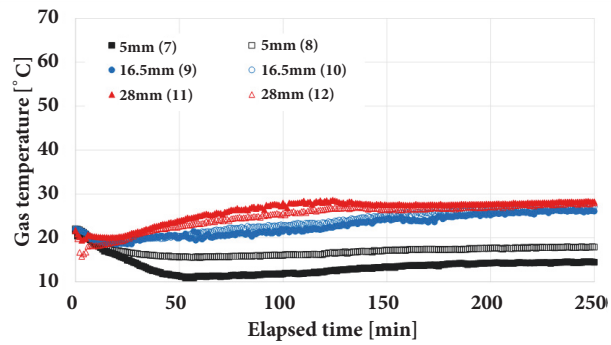

Figure 16: Gas temperature change between inner and outer cylinders (heat input is 324 W). (Distance from bottom of apparatus = 205 mm.)

fluctuated from 0.02 to 0.05 m/s just after the valve opened. Afterward the velocity was stable at 0.03 m/s after about 20 minutes. Finally, it increased to 0.04 m/s. Then, the very weak natural circulation of gas mixture will produce through the cylinder. Helium which filled the top of the cylinder will diffuse downward in the cylinder. Therefore, the mole fraction change in the various parts of the cylinder becomes complicated. We are now carrying out the measurement of the mole fraction and flow velocity by adding the sampling points.

4. Conclusions

We carried out experiments to investigate the mixing processes of two component gases. The conclusions are as follows.

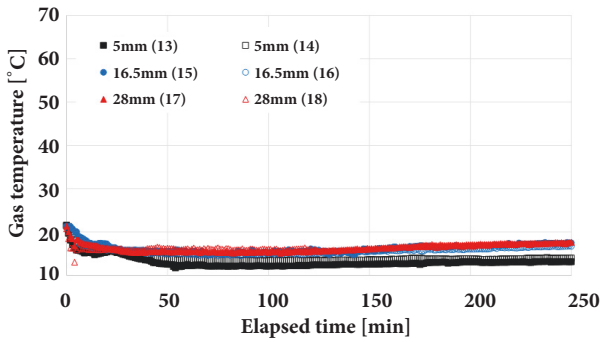

Figure 17: Gas temperature change between inner and outer cylinders (heat input is 324 W). (Distance from bottom of apparatus = 72.5 mm.)

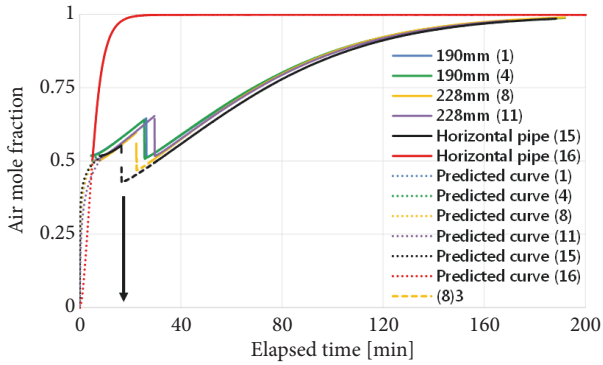

Figure 18: Mole fraction change of air.

The onset time of natural circulation depended more on molecular diffusion than the strength of localized natural convection when the temperature difference was small. On the other hand, the onset time of natural circulation depended not only on molecular diffusion but also on localized natural convection when the temperature difference was large. When not only the localized natural convection but also natural circulation was produced, the onset time of natural circulation becomes short. Therefore, it is important to know whether the localized natural convection or circulation is produced.

After opening the valve of the horizontal double coaxial pipe, air enters the cylinder by a counter-current flow at the outer pipe of the double coaxial pipe. Helium gas which filled the bottom part of the cylinder will be released to the outside of the cylinder. This condition will be terminated immediately. Then, the very weak natural circulation of gas mixture will be produced through the cylinder. Helium gas which filled the top of the cylinder will diffuse downward in the cylinder.

These flow characteristics will be the same as those of phenomena generated in the passage between a permanent reflector and a pressure vessel wall of the VHTR. In order to confirm these results, we are planning to analyze the air ingress phenomena that occur during a depressurized

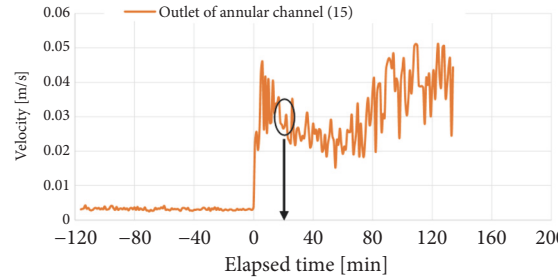

Figure 19: Velocity change.

accident in the GTHTR-300C system. In addition to that, we also are planning to carry out simulations for when the primary pipe of the GTHTR-300C ruptures.

There is no limitation to the use of the experimental data described in this paper.

Nomenclature

Ra_d: Rayleigh number based on the width of the left side slot
Gr_d: Grashof number based on the width of the left side slot
g: Gravity acceleration [m/s^2]
β: Coefficient of volume expansion [1/K]
ΔT: Temperature difference between heated wall and cooled wall [K]
L: Representative length (= width between heated wall and cooled wall) [m]
ν: Kinematic viscosity coefficient[m^2/s]
Pr: Prandtl number
μ: Viscosity coefficient [kg/m·s]
C_p: Constant pressure specific heat [J/kg·K]
λ: Thermal conductivity [W/m·K]
D_{AB}: Mutual diffusion coefficient [cm^2/s].

Data Availability

The data used to support the findings of this study are available from the corresponding author upon request.

Conflicts of Interest

The authors declare that they have no conflicts of interest.

Acknowledgments

A part of this work was supported by JSPS KAKENHI Grant Number JP16K14535.

References

[1] X. Yan, K. Kunitomi, T. Nakata, and S. Shiozawa, "GTHTR300 design and development," *Nuclear Engineering and Design*, vol. 222, no. 2-3, pp. 247–262, 2003.

[2] X. L. Yan, T. Takeda, T. Nishihara, K. Ohashi, K. Kunitomi, and N. Tsuji, "A study of air ingress and its prevention in HTGR," *Nuclear Technology*, vol. 163, no. 3, pp. 401–415, 2008.

[3] T. Takeda and M. Hishida, "Study on the passive safe technology for the prevention of air ingress during the primary-pipe rupture accident of HTGR," *Nuclear Engineering and Design*, vol. 200, no. 1, pp. 251–259, 2000.

[4] C. H. Oh and E. S. Kim, "Air ingress analysis: part 1-theoretical models," *Nuclear Engineering and Design*, vol. 241, pp. 203–212, 2011.

[5] C. H. Oh, H. S. Kang, and E. S. Kim, "Air-ingress analysis: Part 2 - Computational fluid dynamic models," *Nuclear Engineering and Design*, vol. 241, no. 1, pp. 213–225, 2011.

[6] T. Takeda, X. Yan, and K. Kunitomi, "Numerical analysis on air ingress behavior in GTHTR300-cogeneration system," *Journal of Power and Energy Systems*, vol. 1, no. 1, pp. 24–35, 2007.

[7] T. Takeda, "Air ingress phenomena in a depressurization accident of the very-high-temperature reactor," *Nuclear Engineering and Design*, vol. 240, no. 10, pp. 2443–2450, 2010.

[8] T. Takeda and M. Hishida, "Study on diffusion and natural convection of two-component gases," *Nuclear Engineering and Design*, vol. 135, pp. 341–354, 1992.

[9] T. Takeda and M. Hishida, "Studies on molecular diffusion and natural convection in a multicomponent gas system," *International Journal of Heat and Mass Transfer*, vol. 39, no. 3, pp. 527–536, 1996.

[10] C. H. Oh et al., "Thermal hydraulics of the very high temperature gas cooled reactor," in *Proceedings of the 13th International Topical Meeting on Nuclear Reactor Thermal-Hydraulics (NURETH-13)*, Kanazawa, Japan, September 2009.

[11] T. Takeda et al., "Effectiveness of natural convection on molecular diffusion of two component gases in a vertical fluid layer," in *Proceedings of the HTR2010*, paper 038, Prague, Czech Republic, October 2010.

[12] T. Takeda, H. Isomi, H. Hanazawa, and H. Mizuno, "Effectiveness of natural circulation on molecular diffusion of two component gases in a stratified fluid layer," in *Proceedings of the 19th International Conference on Nuclear Engineering (ICONE19-43586)*, Osaka, Japan, October 2011.

[13] T. Takeda and S. Funatani, "Study on air ingress phenomena during a depressurization accident of a VHTR," in *Proceedings of the High Temperature Reactor Technology (HTR '16)*, paper 18632, Caesars Palace, Las Vegas, NV, USA, November 2016.

[14] T. Takeda and S. Funatani, "Development of prevention method for air ingress during a depressurization accident of the VHTR," in *Proceedings of the 24th International Conference on Nuclear Engineering, ICONE24-60990*, Charlotte, NC, USA, June 2016.

[15] T. Takeda, H. Mizuno, and S. Funatani, "Study on mixing process of two component gases in a vertical fluid layer," *Nuclear Engineering and Design*, vol. 271, pp. 424–430, 2014.

[16] T. Takeda, "Mixing process by natural convection and molecular diffusion of two component gases in a stable stratified fluid layer," in *Proceedings of the International Conference on Advanced Power Plant*, paper 8146, Anaheim, Calif, USA, June 2008.

[17] E. R. G. Eckert and W. O. Carlson, "Natural convection in an air layer enclosed between two vertical plates with different temperatures," *International Journal of Heat and Mass Transfer*, vol. 2, no. 1-2, pp. 106–120, 1961.

[18] R. C. Reid, J. M. Prausnitz, and T. K. Sherwood, *The Properties of Gases and Liquids*, McGraw-Hill, New York, NY, USA, 3rd edition, 1977.